CONTROL AND NON-LINEAR COMPENSATION OF A ROTOR/MAGNETIC BEARING SYSTEM SUBJECT TO BASE MOTION

M. O. T. Cole,[1] P. S. Keogh,[1] C. R. Burrows[1]

ABSTRACT

In this paper a study is undertaken which compares the suitability of controllers for a magnetic bearing/rotor system in which motion of the system base can occur. It is demonstrated that controllers which have been selected for directly forced vibration control without consideration of this type of disturbance may give unacceptably poor performance when motion of the base occurs. A method is outlined for designing controllers to give optimal performance for combined base motion and direct rotor forcing disturbances. Controllers were implemented on a flexible rotor/magnetic bearing rig, the base of which was subjected to impulse inputs. The results obtained indicate that motion of the system base, when of sufficient magnitude, can drive the system into a state where magnetic bearing control force saturation occurs. To obtain improved performance a method of on-line compensation was used to linearise the control force characteristics. The results presented in this paper provide a foundation for the controller design of flexible rotor/magnetic bearing systems in applications that induce base motion. These would include transport environments, situations where the system is part of a larger vibratory structure, or in cases where seismic events can occur.

NOTATION

$\mathbf{A}$	system matrix	k_i	PID integral gain
$\mathbf{B}_b, \mathbf{B}_f, \mathbf{B}_u$	state input distribution matrices	k_p	PID proportional gain
c_d	PID derivative gain	s	Laplace transform variable
$\mathbf{C}_y$	output matrix	u_c	magnetic bearing control force
$\mathbf{D}_b$	output matrix	$\mathbf{u}_c$	vector of magnetic bearing control forces
$\mathbf{f}$	vector of direct rotor forces		
f_b	total bearing force	$\mathbf{W}_{\alpha\beta}$	output, input weighting transfer function matrix
$\mathbf{G}$	closed loop transfer function matrix	$\mathbf{x}$	state vector
$\mathbf{G}_b, \mathbf{G}_f, \mathbf{G}_u$	system transfer function matrices	$\mathbf{y}_b$	vector of bearing translatory base motion
$\mathbf{H}$	controller transfer function matrix	$\mathbf{y}_s$	vector of sensor measurement states
$\mathbf{I}_{nxn}$	identity matrix, size n by n	z	relative rotor displacement at bearing
i_c	magnetic bearing control current	ω_b	PID break point frequency
K_i	inherent magnetic bearing current gain	Ω	rotational frequency
K_z	inherent magnetic bearing stiffness		

[1]Department of Mechanical Engineering, Faculty of Engineering and Design, University of Bath, Bath BA2 7AY, UK, tel.: 00 44 1225 826826 x5958, fax: 00 44 1225 826928, e-mail: enspsk@bath.ac.uk.

1 INTRODUCTION

There is a trend towards increased use of magnetic bearings in rotating machinery. The contactless support provided by the bearings allows high speed frictionless operation and active control can be used to attenuate rotor vibration and force transmission. Typically, the method of bearing control is selected to achieve low levels of rotor vibration at the running speed(s) and a reasonable level of damping of the system modes. The simplest way to achieve this is to use local PID feedback at each bearing. Control methods have also been developed that effectively minimise the synchronous rotor vibration, both in open loop (Burrows and Sahinkaya, 1983) and closed loop schemes (Herzog et al., 1996). A common problem with many control schemes is that optimum control at one running speed may prove ineffective or even unstable at another. This is due to rotor gyroscopic effects that increase proportionately with running speed. Methods to overcome this problem have included gain scheduling, for both multi-variable (Sivrioglu and Nonami, 1996) and synchronous control (Knospe, Tamer and Lindlau, 1997). On-line identification methods have also been used with synchronous vibration control (Keogh, Burrows and Berry, 1996). At present many of these control methods have not been qualified in situations where motion of the system base occurs. The problem of using electromagnetic actuators for externally induced vibration absorption has been considered for a two degree of freedom mass system, by (Okada, 1977) and more recently by (Jagadeesh, Simhadri and Stephens, 1997) with their work on electromagnetic absorbers (EMAs). For large base input accelerations with broad frequency content, or when base motion and direct forcing occur simultaneously, a different approach is required. The use of frequency domain control design methods makes it possible to achieve optimised control in this instance.

In this paper, controller performance in response to base motion is compared for controllers that have been selected for directly forced rotor vibration attenuation alone and those that have been designed with consideration of base input disturbances. The controllers include both PID and higher order state space controllers, with and without on-line non-linear compensation of control force. Base inputs are considered that are capable of causing rotor collision with retainer rings under PID control.

2 SYSTEM DESCRIPTION AND MODELLING

The formulation of a flexible rotor/magnetic bearing system as a system of linear differential equations, usually using finite element methods, is well documented. Extension of the flexible rotor model to include magnetic bearings that can move in space, with the system base, gives a first order dynamic equation of the form:

$$\begin{aligned} \dot{\mathbf{x}} &= \mathbf{A}\mathbf{x} + \mathbf{B}_u\mathbf{u}_c + \mathbf{B}_f\mathbf{f} + \mathbf{B}_b\mathbf{y}_b \\ \mathbf{y}_s &= \mathbf{C}_y\mathbf{x} + \mathbf{D}_b\mathbf{y}_b \end{aligned} \tag{1}$$

where $\mathbf{x}$ is a vector of system dynamic states, $\mathbf{u}_c$ is the control force input at the bearings, $\mathbf{f}$ is a vector of disturbance forces acting directly on the rotor, $\mathbf{y}_b$ is the vector of base position (in an inertial frame) and $\mathbf{y}_s$ is a vector of measured rotor displacements relative to the base. In this model, motion in an axial sense is not considered. This formulation is generic for a rotor/magnetic bearing system and may be used for predicting the performance of the experimental system, and also for the synthesis of state space controllers.

For the purposes of control design and analysis, the system can be represented in block diagram form (see figure 1). The open loop system and controller are given as the

transfer function matrices $\mathbf{G}(s)$ and $\mathbf{H}(s)$ respectively, where $\mathbf{G}(s)$ can be obtained from equation (1):

$$\begin{bmatrix} \mathbf{Y}_s(s) \\ \mathbf{U}_c(s) \end{bmatrix} = \mathbf{G}(s) \begin{bmatrix} \mathbf{Y}_b(s) \\ \mathbf{F}(s) \end{bmatrix} \tag{2}$$

where

$$\mathbf{G} = \begin{bmatrix} (\mathbf{I}+\mathbf{G}_u\mathbf{H})^{-1}\mathbf{G}_b & (\mathbf{I}+\mathbf{G}_u\mathbf{H})^{-1}\mathbf{G}_f \\ \mathbf{H}(\mathbf{I}+\mathbf{G}_u\mathbf{H})^{-1}\mathbf{G}_b & \mathbf{H}(\mathbf{I}+\mathbf{G}_u\mathbf{H})^{-1}\mathbf{G}_f \end{bmatrix} \tag{3}$$

and

$$\mathbf{G}_u(s) = \mathbf{C}_y(s\mathbf{I}-\mathbf{A})^{-1}\mathbf{B}_u \tag{4}$$

$$\mathbf{G}_f(s) = \mathbf{C}_y(s\mathbf{I}-\mathbf{A})^{-1}\mathbf{B}_f \tag{5}$$

$$\mathbf{G}_b(s) = \mathbf{C}_y(s\mathbf{I}-\mathbf{A})^{-1}\mathbf{B}_b + \mathbf{D}_b \tag{6}$$

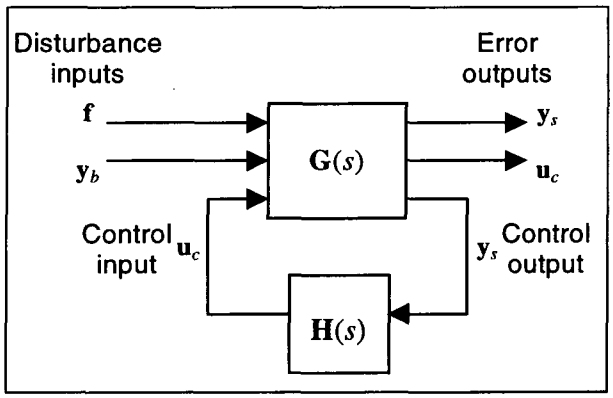

Figure 1. System representation for control problem

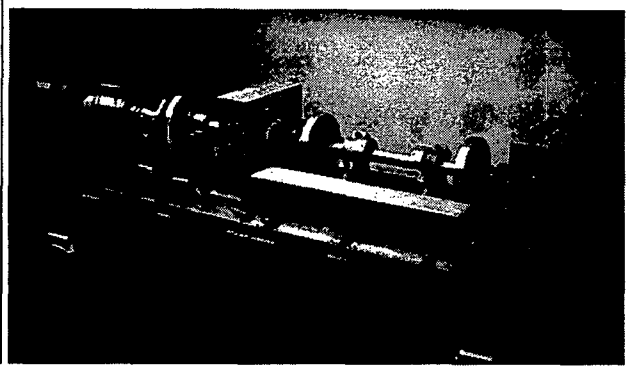

Figure 2. Flexible rotor / magnetic bearing rig

3 EXPERIMENTAL FACILITY

The rig used for the implementation and testing of the controllers is shown in figure 2. This facility was designed and manufactured to allow comprehensive testing of a generic flexible rotor/magnetic bearing system. The rotor comprises a 2m shaft with four disks, supported by two radial magnetic bearings. Each bearing has two opposing coil pairs, giving a total of four control force axes. The rotor displacement, relative to the base frame, is measured in four planes using four pairs of eddy current displacement transducers. Two pairs of these sensors are local to the bearings and are used for local PID feedback. However, all eight sensors can be used as multivariable control inputs. Two retainer bearings, having radial clearance of 0.7 mm, are situated in each bearing housing. Four bronze retainer rings, of radial clearance 0.8 mm, are also positioned at four rotor locations. Eight switching current amplifiers control the current through the magnet coils. Bearing characteristics are described further in section 5.

The control software, programmed in C++, is implemented on a PC based digital signal processor. This has two main interrupt routines; one for the PID controller and one for the state space controller (when running). The speed of the processor is sufficient to allow state space controller of up to 50 states, as well as the execution of numerous auxiliary tasks.

Motion of the system base is produced by an impact mechanism which imparts a horizontal impulse to the base. The resulting oscillatory motion comprises mainly the

horizontal rigid body mode frequencies of the base; 25 rad/s (4 Hz) for the translatory mode and 44 rad/s (7 Hz) for the yawing mode. Changing the position of the impact allows control over the level of excitation of each mode. Though the system is not truly linear, the motion of the rotor while rotating will approximate to a linear superposition of the synchronous and non-rotating base motion response. The bandwidth of the base impulse is tuned to be approximately 100 rad/s, which is significantly lower than the rotor first bending mode. The same magnitude of base impulse was used for all testing in this study.

4 PID CONTROL

Although digitally implemented, the PID control law takes the standard form in the Laplace domain:

$$\mathbf{H}(s)=\left(\frac{k_i}{s}+k_p+\frac{c_d\omega_b s}{s+\omega_b}\right)\mathbf{I}_{4x4} \tag{7}$$

where k_i is the integral component gain, k_p the proportional gain and c_d the derivative component gain. The frequency ω_b is the break point for the derivative action. Typically, digital implementation of the controller, in state space form, is accomplished with a sampling frequency of 3000 Hz. The fast sampling period allows direct conversion of controllers from the Laplace domain to the Z domain, for digital implementation, using a zero order hold conversion. There exists standard methods for choosing appropriate values for the PID parameters. However, selection based on one criteria alone may be unsuitable for the type of system (equation (1)) considered in this study.

4.1 PID EXPERIMENTAL RESULTS

Figure 3(a) shows the rotor synchronous response for a typical PID controller (equation (7)) with k_p = 2.7x10^6 N/m, c_d = 2500 Ns/m, k_i = 0.1x10^6 N/ms and ω_b = 1500 rad/s. The outer sensor response shows the motion at the non-driven end disk and the inner sensor shows the motion at the non-driven end bearing. Three critical speeds are clearly visible, corresponding to the two predominantly rigid body modes (at 40 and 80 rad/s) and to the rotor's first bending mode (at 180 rad/s). The rotor was then stopped and an impulse applied horizontally to the base at the non-driven end bearing location. The response with this controller is shown in figure 4(a). It is evident that contact of the rotor with the retainer bearings has occurred during four oscillations following impact and the relative rotor to base motion took over two seconds to decay. In order to reduce the base motion response, the PID proportional gain was increased to 3.4x10^6 N/m to give stiffer bearings. This clearly improved the response of the rotor (figure 4(b)) and retainer bearing contact did not occur. However, the effect of increasing stiffness on the synchronous response is clearly detrimental (figure 3(b)). Increasing bearing stiffness increases the modal frequencies but reduces the modal damping and so peak amplitudes at resonance are notably increased. Modal damping could be improved by increasing derivative feedback at the bearings (i.e. increasing c_d). However, this can cause problems of poor noise attenuation and possible control force saturation, depending on the performance of the system power electronics.

Either of the PID controllers in figure 3 would yield an acceptable synchronous response at a rotational speed of 150 rad/s. Figure 5 shows the base excited response of the rotor at this speed. The bandwidth of the base impulse causes mainly rigid body motion superimposed with the synchronous response. A sharper impulse would excite higher order flexible rotor modes.

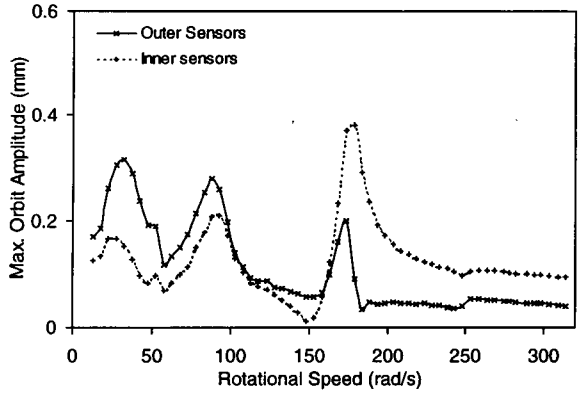

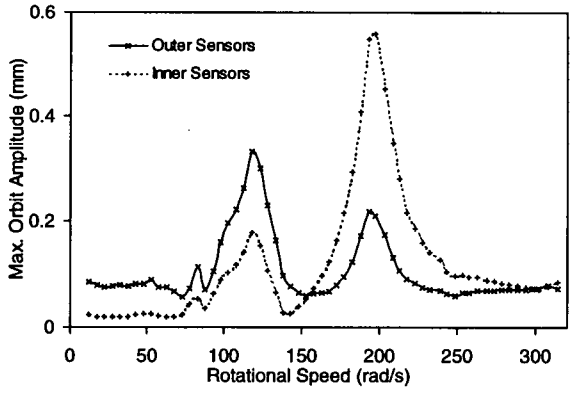

Figure 3. Synchronous response for PID controllers
(a) Low stiffness $k_p = 2.7\text{x}10^6$ N/m **(b) High stiffness $k_p = 3.4\text{x}10^6$ N/m**

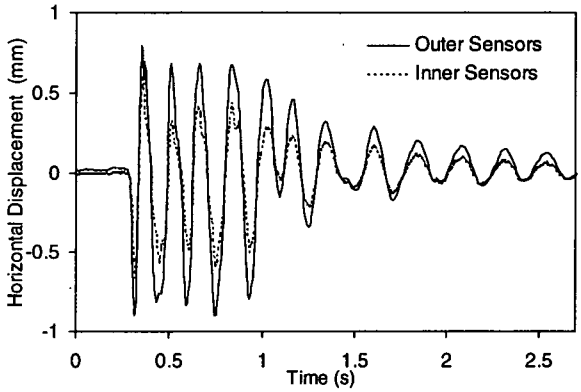

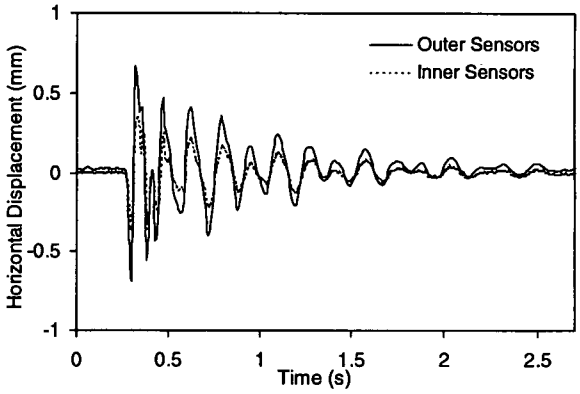

Figure 4. Base input response for PID controllers
(a) Low stiffness $k_p = 2.7\text{x}10^6$ N/m, $\Omega = 0$ rad/s **(b) High stiffness $k_p = 3.4\text{x}10^6$ N/m, $\Omega = 0$ rad/s**

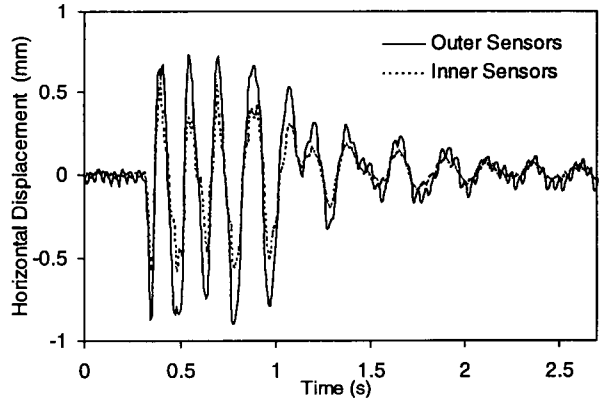

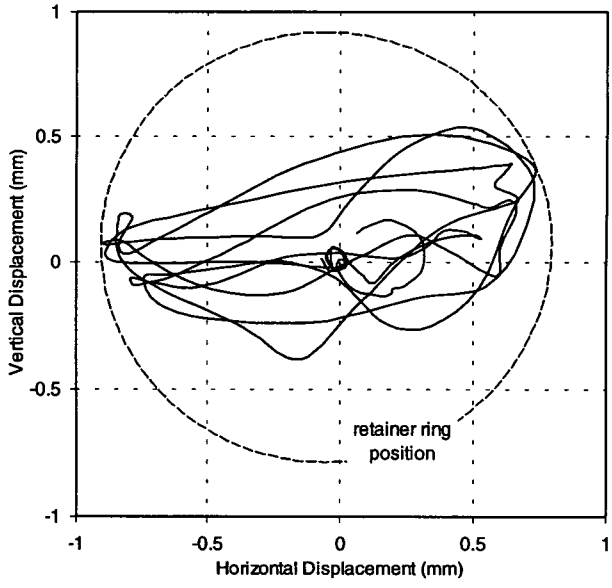

Figure 5. Base input response for low stiffness PID controller, $k_p = 2.7\text{x}10^6$ N/m, $\Omega = 0$ rad/s
(a) Horizontal displacement only **(b) Rotor path at outer sensors over 1 second following impact**

5 NON-LINEAR BEARING CHARACTERISTICS

Theoretical magnetic bearing force-current-displacement characteristics can be obtained from the modelling of magnetic flux distribution. A viable alternative, used for this system, is direct measurement of bearing force characteristics. This is accomplished on the individual bearings and cores prior to the system assembly. Experimental data is obtained by applying the appropriate bias currents to a single coil pair and measuring the change in force with both displacement (displacement gain K_z) and control current (current gain K_i). Displacement and force are measured along the coil axis only, although a more thorough investigation would involve measurement perpendicular to the coil axis in order to quantify the degree of axis cross-coupling. A plot of the force change with displacement from the bearing centre (figure 6(a)) shows approximate linear dependency (K_z = 1.94x10^6 N/m). A plot of control force against control current (figure 6(b)) shows clear evidence of magnetic saturation for control forces greater than 1000 N. A linear fit over a range ± 1000 N gives a value of K_i = 530 N/A. Both plots show the change in force relative to a constant force bias of 325N, required to support the rotor weight.

Control design and implementation has thus far been achieved assuming a linearised bearing force f_b:

$$\begin{aligned} f_b &= K_z z + K_i i_c \\ &= K_z z + u_c \end{aligned} \tag{8}$$

where, z is the rotor displacement from the bearing centre, i_c is the control current and u_c is the control force. Control currents are calculated on-line as

$$i_c = u_c / K_i \tag{9}$$

5.1 CONTROLLER MODIFICATIONS

Although control force saturation occurs above ± 1000 N, the available control force is in excess of ± 1500 N. Therefore, it is reasonable to expect improved control performance if non-linear compensation of the control force/current relationship is used to linearise the control input over the full range of available force. This is achieved using a cubic polynomial function, derived from figure 6(b), that maps the control current (calculated from equation (9)) to a modified control current i_c':

$$i_c' = i_c + a(i_c + b)^3 \tag{10}$$

The parameters a and b are chosen so that the modified control force gives a good fit to the experimental data. The approximation of bearing characteristics thereby obtained is shown in figure 6(b).

The authors are aware that more comprehensive studies of bearing characteristics have been undertaken (Knight et al., 1996) and that more sophisticated methods of non-linear control have been developed. However, this type of modelling will allow simple quantification of the benefits achievable with non-linear compensation techniques.

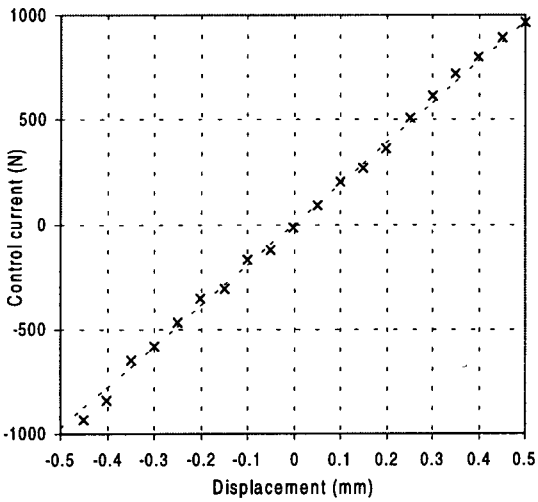

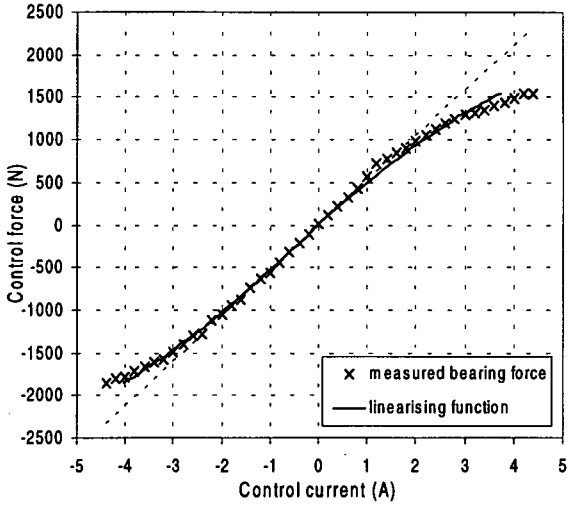

Figure 6. Measured bearing characteristics
(a) Force-displacement with linear fit **(b) Force-current with linear and non-linear fit**

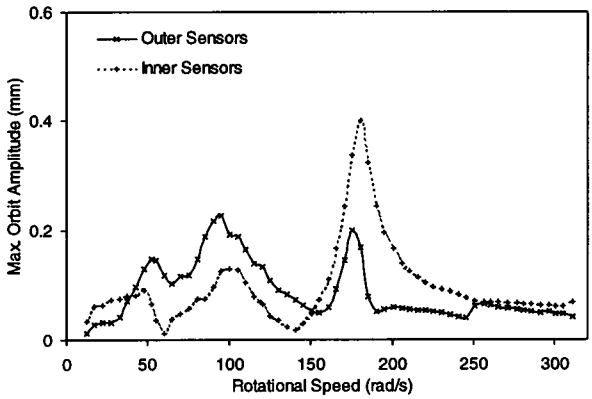

Figure 7. Synchronous response for low stiffness PID controller with non-linear compensation, k_p= 2.7x10^{-6} N/m

5.2 EXPERIMENTAL RESULTS

With the addition of non-linear compensation there is a slight reduction in synchronous vibration amplitude at low rotational speed, most notably for the low stiffness PID controller (figure 7). This can be explained by the softening of stiffness that occurs in the uncompensated system. Figure 8(a) shows that the non-linear compensation improves the base input response significantly for the low stiffness PID controller. Although back up bearing contact still occurs, it is only over two oscillations and the oscillation decays considerably faster than without the non-linear compensation (c.f. figure 4(a)).

Although non-linear compensation can extend the linear regime of the control input, force saturation will still occur, albeit at a higher force level. Also, the transition will be more abrupt. A controller gain that is too high may, therefore, still cause problems associated with control force saturation. For example, the effect of control force saturation, that occurs with the high stiffness PID controller during large amplitude base motion, can contribute to excitation of higher frequency modes (figure 8(b)). Additionally, during synchronous testing the system was found to lose stability on passing through the rotor first critical. This is a direct consequence of abrupt control force saturation.

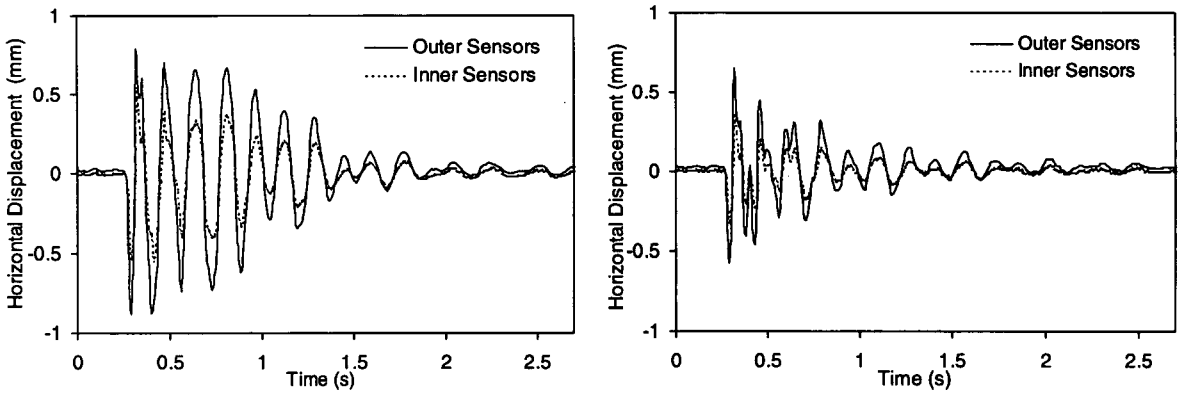

Figure 8. Base input response for PID controllers with non-linear compensation, $\Omega = 0$ rad/s
(a) Low stiffness, $k_p = 2.7\text{x}10^6$ N/m **(b) High stiffness, $k_p = 3.4\text{x}10^6$ N/m**

6 STATE SPACE CONTROL

State space controller design was undertaken to find a controller that minimises the objective function J, a weighted transfer function norm of the closed loop system:

$$J_{\infty,2} = \left\| \mathbf{W}_\alpha(s)\{\mathbf{G}(\mathbf{H})\}(s)\mathbf{W}_\beta(s) \right\|_{\infty,2} \tag{11}$$

where the subscripts ∞ and 2 denote the infinity-norm and 2-norm respectively. This type of control synthesis was used on the full system to simultaneously minimise response to both directly forced and base input rotor disturbances. For purposes of comparison, the synthesis was also carried out without minimisation of the base input response. Input weightings were chosen to reflect the expected frequency content of the disturbances and output weightings to reflect the required frequency response at the system outputs. This design method allows the frequency dependent shaping of transfer function singular values in order to influence performance and control levels (and thereby robustness). A more rigorous account of the state space modelling and linear controller design is given in (Cole, Keogh and Burrows, 1997).

Non-linear compensation is also used with the state-space control to extend the regime of linear behaviour. Although this has minimal effect under purely synchronous excitation, as control force levels remain small, it should help reduce base excited motion during large transients.

6.1 EXPERIMENTAL RESULTS

The synchronous response measurements shown in figure 9 compare three different state space controllers. The first controller (SS1) was designed with an H_∞ performance objective (equation (11)) applied to the direct forcing (unbalance) response only. The second controller (SS2) was designed using an H_∞ performance objective on both direct forcing and base motion response while the third (SS3) was designed using an H_2 performance objective on both direct forcing and base motion response. The peak amplitude of the synchronous response is similar for all three controllers and notably better than for the PID controllers. The H_2 controller is actually slightly better than the other two controllers. It is suggested that this is because using an H_∞ objective will minimise the response to the worst case disturbance input, which rarely occurs in practice, whereas the H_2 objective weights all disturbances equally.

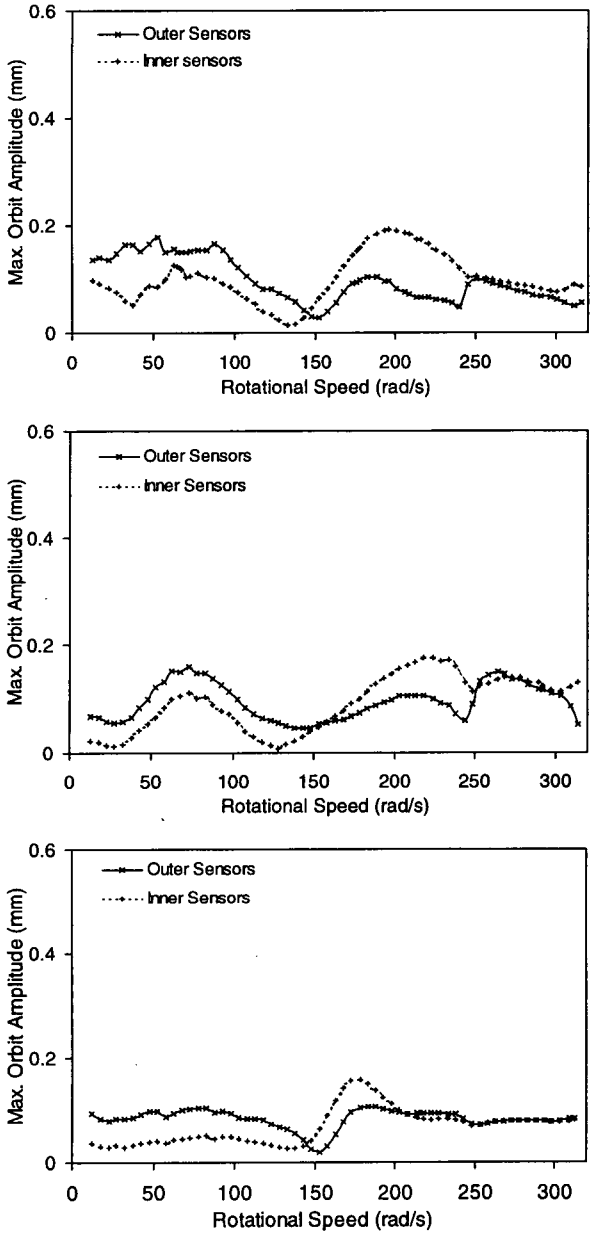

Figure 9. Synchronous response for state space controllers

(a) Controller SS1
(b) Controller SS2
(c) Controller SS3

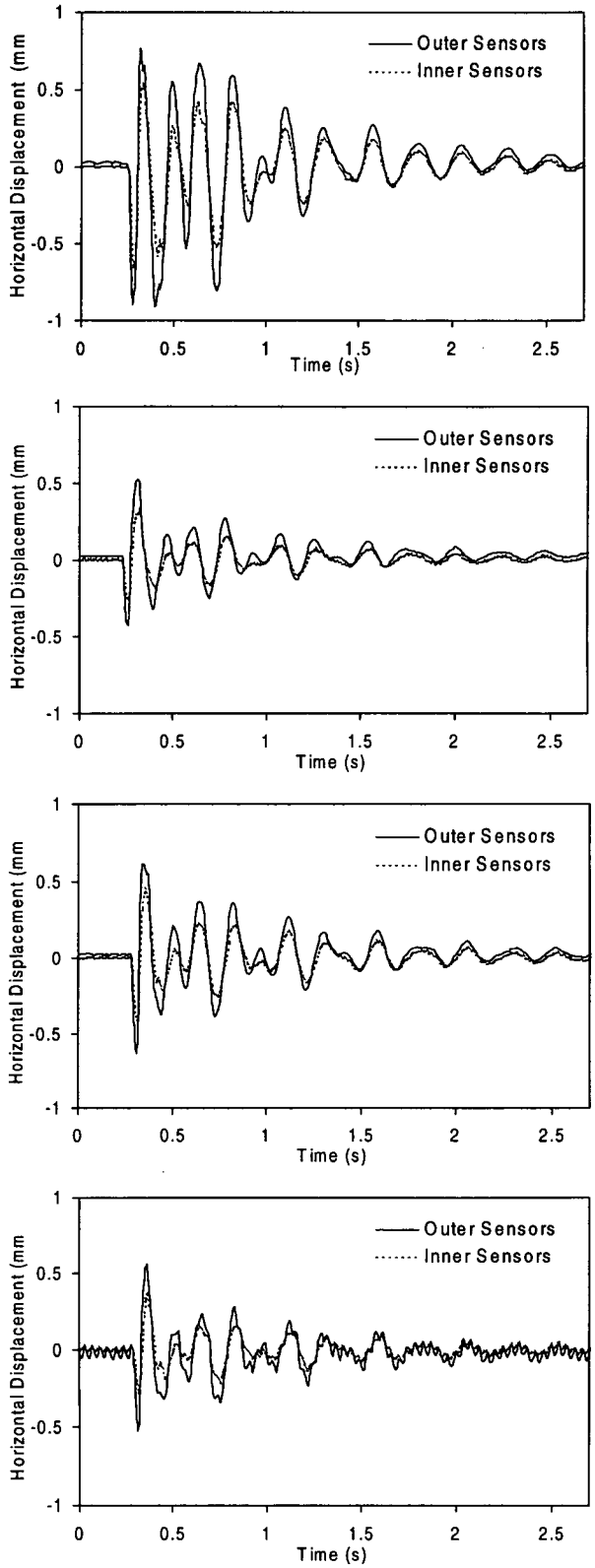

Figure 10. Base input response for state space controllers

(a) Cont. SS1, $\Omega = 0$ rad/s, (b) Cont. SS2, $\Omega = 0$ rad/s
(c) Cont. SS3, $\Omega = 0$ rad/s, (d) Cont. SS3, $\Omega = 150$ rad/s

Figure 10 shows the base input response for the three state space controllers. It is evident that system response is significantly worse when using the controller for which base motion has not been included in the design objective (SS1). However, the controllers designed for base input (SS2 and SS3) give a significant improvement over both the PID controllers and SS1.

7 CONCLUSIONS

It has been demonstrated, through experiment, how controller design can influence the performance of a flexible rotor-magnetic bearing system under conditions of both directly forced and base motion type disturbances. It has been shown that PID controller design may compromise performance with this type of system. However, optimised state space control can give simultaneous attenuation of vibration arising from both types of disturbance. It has also been shown that non-linear control force saturation can limit performance during large amplitude base motion and that non-linear compensation can improve performance and help prevent backup bearing contact in this instance.

ACKNOWLEDGEMENT

The authors acknowledge the support of the Engineering and Physical Sciences Research Council under Grant GR/J15575 and a Research Studentship for M O T Cole.

REFERENCES

Burrows, C.R. and Sahinkaya, M.N. "Vibration control of multi-mode rotor bearing system," *Proceedings, Institution of Mechanical Engineers,* 1983, Part C, Vol. 207, pp.1-17.

Herzog, R., Bühler, P., Gahler, C. and Larsonneur, R., "Unbalance compensation using generalised notch filters in the multivariable feedback of magnetic bearings," *IEEE Transactions on control system technology,* 1996, Vol. 4, No. 5, pp. 580-586.

Sivrioglu, S. and Nonami, K. "LMI approach to gain scheduled H_∞ control beyond PID control for gyroscopic rotor-magnetic bearing system," *Proceedings, 35th Conference on Decision and Control,* 1996, Kobe, pp. 3694-3699.

Knospe, C.R., Tamer, S.M. and Lindlau, J, "New results in adaptive vibration control," *Proc. Mag '97 Industrial conference and exhibition on magnetic bearings*, Virginia, 1997, pp. 209-219.

Keogh, P.S., Burrows, C.R. and Berry, T. "On-line controller implementation for attenuation of synchronous and transient rotor vibration," *ASME Journal of Dynamic Systems, Measurement, and Control,* 1996, Vol. 118, pp. 315-321.

Okada, Y. "Analysis and experiments of the electro-magnetic servo vibration damper," *Bulletin of the JSME,* 1997, Vol. 20, No. 144, pp. 696-702.

Jagadeesh, S., Simhadri, S. and Stephens, L.S. "Design of a 2-DOF electro-magnetic absorber test rig for controller development," *Proceedings, MAG '97, 1997*, Virginia, pp.199-208.

Knight, J.D., Xia Z., McCaul, E. and Hacker H. "Determination of forces in a magnetic bearing actuator: numerical computation with comparison to experiment," *ASME Journal of Tribology,* 1992, Vol. 114 pp.796-801.

Cole, M.O.T., Keogh P.S. and Burrows, C.R. "Vibration control of a flexible rotor/magnetic bearing system subject to direct forcing and base motion disturbances," *Accepted for IMechE, Proceedings Journal (Part C),* submitted 1997.